# Numerical Simulation of Microphysics in Meso-$\beta$-Scale Convective Cloud System Associated with a Mesoscale Convective Complex

*Fan Beifen* (范蓓芬), *Ye Jiadong* (叶家东)
Department of Atmospheric Sciences, Nanjing University, Nanjing 210008

*William R. Cotton* and *Gregory J. Tripoli*①
Department of Atmospheric Sciences, Fort Collins, CO 80523 U.S.A.
Received March 28, 1989

ABSTRACT

Numerical simulation of meso-$\beta$-scale convective cloud systems associated with a PRE-STORM MCC case has been carried out using a 2-D version of the CSU Regional Atmospheric Modeling System (RAMS) nonhydrostatic model with parameterized microphysics. It is found that the predicted meso-$\gamma$-scale convective phenomena are basically unsteady under the situation of strong shear at low-levels, while the meso-$\beta$-scale convective system is maintained up to 3 hours or more. The meso-$\beta$- scale cloud system exhibits characteristics of a multi-celled convective storm in which the meso-$\gamma$-scale convective cells have lifetime of about 30 min. Pressure perturbation depicts a meso-low after a half hour in the low levels. As the cloud system evolves, the meso-low intensifies and extends to the upshear side and covers the entire domain in the mid-lower levels with the peak values of 5-8 hPa. Temperature perturbation depicts a warm region in the middle levels through the entire simulation period. The meso-$\gamma$-scale warm cores with peak values of 4-8℃ are associated with strong convective cells. The cloud top evaporation causes a stronger cold layer around the cloud top levels.

Simulation of microphysics exhibits that graupel is primarily concentrated in the strong convective cells forming the main source of convective rainfall after one hour of simulation time. Aggregates are mainly located in the stratiform region and decaying convective cells which produce the stratiform rainfall. Riming of the ice crystals is the predominant precipitation formation mechanism in the convection region, whereas aggregation of ice crystals is the predominant one in the stratiform region, which is consistent with observations. Sensitivity experiments of ice-phase microphysical processes show that the microphysical structures of the convective cloud system can be simulated better with the diagnosed aggregation collection efficiencies.

## I. INTRODUCTION

Numerous observational evidences have revealed that the ice particle aggregation process is one of the predominant mechanisms of precipitation formation in a variety of cloud systems (Jiusto, 1971; Hobbs et al., 1974; Matejka et al., 1980; Heymsfield and Musil, 1982; Stewart et al., 1984; Houze and Churchill, 1984; Jorgensen, 1984; and Rauber, 1987). Airborne cloud microphysical data obtained from midlatitude mesoscale convective systems (Yeh et al., 1988) also indicated that aggregates comprise an important component of the precipitation in the stratiform region and transition region of midlatitude mesoscale convective complexes (MCC), especially in the stratiform region.

① Current affiliation: University of Wisconsin, Department of Meteorology, Madison, WI 53715

Cotton et al. (1986) developed an aggregation model in the CSU Regional Atmospheric Modeling System (RAMS) and applied it to the simulation of orographic cloud snowfall. The numerical experiments demonstrated that aggregation plays an important role in controlling the fields of cloud liquid water content, ice crystal concentrations, and surface precipitation amounts. Chen (1986) also applied the model to the simulation of the stratiform region of a midlatitude mesoscale convective complex observed on 14–15 July 1984 during the Airborne Investigations of Mesoscale Convective Systems (AIMCS) Experiment in which the microphysical structures in the stratiform region of it have been analyzed by Yeh et al. (1988). The model predicted the general features of the thermodynamics and dynamics of the cloud system, and demonstrated the effects of the long-wave radiation on the enhancement of the internal cloud circulations in the stratiform region of the MCC. However, the simulation results displayed that the ice-crystal category of water species occupied over the whole stratiform region with the maximum ice mixing ratio of 3.4–3.8 g / kg in the mature stage of the MCC, whereas the aggregate category almost did not be found in the stratiform region of the modeling cloud system, which is inconsistent with the observations. The model underpredicted the amount of aggregates over the stratiform region. This deficiency probably is attributed to some incompleted aspects of aggregation model.

In this paper we applied a two-dimensional version of the CSU RAMS nonhydrostatic cloud model with improved parameterized microphysics to the simulation of meso-$\beta$ scale convective cloud system associated with a mesoscale convective complex observed on 4 June 1985 during the PRE-STORM experiment. The microphysical structures in the stratiform region and transition region of the MCC have been analyzed by Yeh et al. (1987).

## II. DESCRIPTION OF MODEL

The Colorado State University (CSU) Regional Atmospheric Modeling System (RAMS) developed by Cotton's group is front-ended by a preprocessor software package which allows the construction of a Fortran code that is one-dimensional, two-dimensional, or three dimensional and utilizes various options in dynamics, thermodynamics and microphysics. The governing equations and general features of the model system are described in Tripoli and Cotton (1982), Cotton et al. (1982) and Cotton et al. (1986). In this case we used a two-dimensional, nonhydrostatic, time-dependent cloud model with parameterized microphysics to the simulation of a meso-$\beta$ scale convective system. Several aspects of the aggregation model developed by Cotton et al. (1986) have been improved in the new version of parameterized microphysics. We shall describe here the improvements in the aggregation model.

### 1. *Empirical Estimation of Aggregation Efficiency of Ice Particles*

One of the main problems in the simulation of snowflake aggregation is the collection efficiency between ice crystals, which is the product of the collision efficiency and the adhesion efficiency. The collision efficiency is determined by the aerodynamics associated with the flow of air around the collision particles, which is complicated by the nonuniform vertical and horizontal motions of ice particles. The adhesion mechanism is also a complicated process affected by a variety of factors such as the air temperature, humidity, crystal habits, and the presense of supercooled cloud droplets.

Hallgren and Hosler (1960) measured the collection efficiencies of ice particles in the laboratory and showed at ice saturation the collection efficiencies were low, usually less than 0.2, and decreased as the temperature decreasing from −11℃ to −26℃. Between −11℃ and

−6℃ they decreased with increasing temperature. Latham and Saunders (1971) showed from their experiments, that the collection efficiencies at ice saturation were approximately constant at about 0.3. On the other hand, Passarelli (1978) deduced a mean aggregation efficiency of $1.4 \pm 0.6$ from aircraft data, over the temperature range from −12℃ to −15℃ . The difference between Passarelli's findings and that obtained from laboratory studies was probably due to the fact that more elaborate crystal shapes and a broader spectrum of crystal sizes plus higher levels of turbulence are found in natural clouds than that in the laboratory. Moreover, most studies were carried out at ice saturation which is probably different with the most situations in the natural clouds. Hosler et al. (1957) noted that considerably higher efficiencies were measured at ice supersaturation such as occurs in a natural cloud containing supercooled cloud droplets.

We therefore applied Passarelli's (1978) scheme to diagnose the collection efficiency in the stratiform region of the PRE–STORM MCC case observed on 4 June 1985 during its mature stage. Passarelli applied the moment conservation equations for the total mass and reflectivity factor fluxes for aggregating snowflakes to calculate the mean collection efficiency. For the case of steady, constant snow mass flux, the resulting explicit expression of the mean collection efficiency $\bar{E}$ in a layer is

$$\bar{E} = (\lambda^{-1-b} - \lambda_0^{-1-b}) \frac{12\Gamma(7+b)\lambda^{4+b}}{(1+b)\pi N_0 h I(b)} , \tag{1}$$

where $h$ is the height below a reference level $(z=0)$, $N_0$ and $\lambda$ are the size distribution parameters of exponential distribution at $z=h$, $\lambda_0$ is the slope parameter of the size distribution at the reference level $(z=0)$, and $b$ is a parameter in the particle falling speed equation:

$$v(D) = aD^b \tag{2}$$

and

$$I(b) = \int_0^\infty \int_0^\infty x^3 y^3 (x+y)^3 |x^b - y^b| e^{-(x+y)} dx dy. \tag{3}$$

Based on the experiments of Hobbs et al. (1974), we selected $b=0.25$, then integrating equation (3) obtained $I(b) = 566$. Thus, based on the assumption of constant mass flux, the mean collection efficiency in a certain layer can be calculated from Eq. (1) when the particle size distribution parameters $N_0$ and $\lambda$ are known at the layer boundaries.

We calculated the values of the size distribution parameters $N_0$ and $\lambda$ at various levels based on the data observed in the location $A$ of the stratiform region of the MCC observed on 4 June 1985 as shown in Yeh et al(1987). We remember that during the time of the vertical sounding carried out at the location A, and cloud system is in its mature stage, and the aircraft was descending slowly with a similar style of termed advecting spiral descent suggested by Lo and Passarelli (1982) through the stratiform region with a descending speed of about 1–2 $ms^{-1}$ to trace the growth process of the aggregates, so the assumption of constant mass flux of snowflakes is reasonably satisfied here. The best fit lines for $N_0(z)$ and $\lambda(z)$ exhibit the correlation coefficients of 0.76 and 0.54 as shown in Fig. 1, respectively. The empirical relations are given by

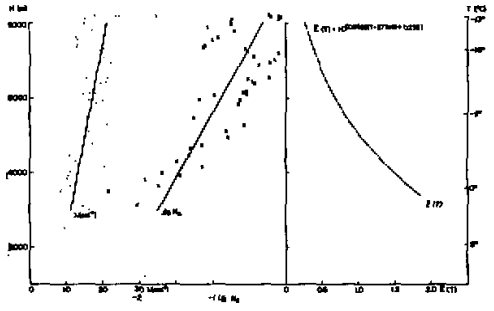

*Fig. 1.* Scatter diagrams of slope parameter $\lambda$ and intercept parameter $N_0$ of Marshall–Palmer distribution of hydrometeor size spectra at various levels and corresponding empirical aggregation efficiency as a function of temperature calculated from Passarelli's method (1978).

$$N_0(z) = 1.9 \times 10^{-4} 10^{0.56z} \tag{4}$$

$$\lambda(z) = -2.30 + 3.89z, \tag{5}$$

where $z$ is in km, $N_0$ and $\lambda$ are in $\mathrm{cm}^{-4}$ and $\mathrm{cm}^{-1}$ respectively. Using the relations the mean collection efficiencies at various layers have been calculated. We obtained an empirical formula as

$$\overline{E(T_s)} = 10^{0.235 + 0.0633T_s} \tag{6}$$

with a fitting correlation coefficiency of 0.98, or, a simpler linear relation as

$$\overline{E(T_s)} = 1.627 + 0.128T_s \tag{7}$$

with a correlation coefficiency of 0.96, where $T_s = T - 273.16$, and $T$ represents the diagnosed surface temperature of the ice particle. This empirical relation is available in the temperature range from 0℃ to −13℃ in which the microphysical data obtained. The Hallgren and Hosler's results with the temperature dependent coalescence efficiency formula:

$$\overline{E(T_s)} = min[10^{0.035T_s - 0.7}, 0.2], \tag{8}$$

was still used beneath −13℃ which is similar with Cotton et al. (1986).

2. *The Conversion Term from Aggregates to Graupel*

The conversion from aggregates to graupel can happen by aggregate collecting cloud droplets which should result in a concentration tendency for aggregate, graupel and cloud droplet. The calculation is actually made in two parts. The first part is the conversion of cloud droplets to aggregates, i.e., the riming tendency. Then we convert from aggregates to graupel based on that riming tendency. The problem is, however, how much rimed aggregates will be really converted to graupel? This is a difficulty because certainly an aggregate can rime some cloud droplets and still be called an aggregate until some critical point is reached where we start calling it graupel. Since when we see a distribution of aggregates we do not know how much rime they have, we cannot make that decision. One of the approaches to solve the problem approximately is that the total mass of aggregates probably will not become graupel without some significant riming. So, if we require a criterion riming degree not to be exceeded, we can put the excess into conversion. This would only make graupel from aggregates in very vigorous cases. We suggest the rate could be that amount in excess of the deposi-

tion and ice crystal collection rates. The physical reasoning being that if riming is a dominant growth process, then the rimed aggregates start looking like graupel. Therefore, we obtain the conversion term from aggregates to graupel as

$$CN_{ag} = [\max(CL_{ca} - (CL_{ia} + CL_{sa} + VD_{va}),0.) + CL_{ar}]H(T_s), \quad (9)$$

where $CN_{ag}$ is the conversion rate from aggregates to graupel, $CL_{ca}$ is the riming rate of aggregates, $CL_{ia}$, $CL_{sa}$ and $CL_{ar}$ are the collection rates of pristine crystal, snow crystal and raindrop with aggregates, respectively, $VD_{va}$ is the deposition rate of vapor on the aggregates, and $H(T_s)$ is the Heaviside step function.

## III. THE PRE-STORM CASE of 4 JUNE 1985

The case selected for simulation is a meso-$\beta$ scale convective cloud system associated with a PRE-STORM MCC of 4 June 1985. The MCC developed in association with a short wave trough system which passed through mid-west region of the United States. An associated cut-off low pressure center was located over southern California which is evident from 700 hPa to 300 hPa levels (Figure omitted). A southwest air current was prevalent to the east of the trough and the low center above 700 hPa level, which brought the warm and drier air to the area of PRE-STORM network. At 850 hPa level, a 13-15 $ms^{-1}$ southerly jet pumped warm moist Gulf air northward through central Texas, across the surface front at about the Oklahoma-Kansas border, towards the Panhandle of Texas, northwest Oklahoma, and the western sections of Kansas and Nebraska. The synoptic situation is favorable for the set up of the instability in the mid-low levels of atmosphere and the development of a mesoscale convective system.

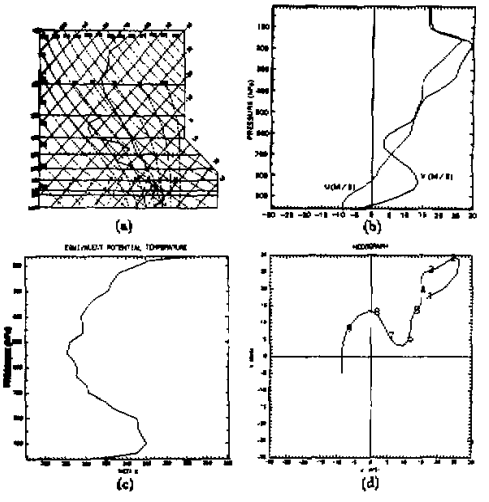

Fig. 2. Vertical profiles of thermodynamics and horizontal wind components $u$ and $v$ for initial sounding from Wichita, Kansas at 06 GMT, 4 June 1985. (a) skew $T - \log P$ diagram, (b) equivalent potential temperature, (c) horizontal wind component $u$ and $v$ profiles (d) hodograph of horizontal winds.

Figure 2 shows an analyzed result of the sounding data taken from Wichita at 0600 GMT just before the MCC developing which was used to initialize the model simulations.

Some important features are revealed: 1) The atmosphere was warm and moist in the low levels, and dry in the middle troposphere; 2) A southern low level warm moist jet of 13–15 $ms^{-1}$ was near 850 hPa level, and a southwestern upper level jet of about 40 $ms^{-1}$ near 200 hPa level (Fig. 2b); 3) A deep conditional instable layer was from 900 hPa level up to 500 hPa level (Fig. 2c); 4) the wind hodograph displayed that wind veer shear was evident beneath the 600 hPa level, above it the southwest air current prevailing until up to 100 hPa level (Fig. 2d).

The MCC was a rapidly evolving and fast moving, non–linear system, which formed by 0630 GMT and dissipated at about 1400 GMT. In the early time of its lifecycle, numerous convective cells developed in a random manner. At 0800 GMT the convective echoes started to organize into several meso–$\beta$ scale sub–systems (Fortune and McAnnelly, 1986). The propagation speeds of the MCC were about 15–25 $ms^{-1}$ from the direction of about 270°. Under the influence of low level convergence and low level southern jet which located at the western side of the storm system at the 850 hPa level, the meso–$\beta$–scale sub–systems moved with various direction and speed. In the southwest part, some meso–$\beta$–scale convective clusters waved to 60° with speeds of 15–20 $ms^{-1}$, and some northern subsystem moved to east. Some of the meso–$\beta$–scale convective cloud systems lasting more than 3 hours although the convective action in it have decayed within its 3 hours lifetime. We focus on the simulations of the meso–$\beta$ scale convective cloud system. Airborne observations have revealed as described on Yeh et al, (1987) that the characteristics of ice particle are quite different between the stratiform region and transition region of the MCC. Most of the large particles are aggregates and graupel particles in the transition region, whereas aggregates predominate in the stratiform region. The aggregation process in the stratiform region started at upper and colder levels but become more efficient as the aggregates approach the melting layer.

## IV. DESIGN OF NUMERICAL EXPERIMENT

### 1. *Model Domain and Grid Points, Boundary Conditions and Initial Conditions*

The two dimension model domain was 90 km long and 19 km high with a grid resolution of $\Delta x = 1$ km and $\Delta z = 0.5$ km. The $x$–coordinate was selected pointing 60° from north, which is basically parallel to the wind shear vector from surface to 600 hPa level. The coordinate frame moved with an average speed of 15 $ms^{-1}$ along the $x$–axis. A 10 s time step was used in the simulation for the first hour, and 7.5 s after. The radiative lateral boundary condition and normal mode radiative top boundary condition were used in the simulation as applied in the orograph cloud simulation by Cotton et al. (1986). A cold downdraft initialization method which attempts to model evaporative cooling from an initial cell is used to trigger the cloud circulation. The model was initialized using the sounding data taken from Wichita at 0600 GMT 4 June 1985 just before the MCC developed. In addition, a mesoscale updraft was applied in the simulation beneath 6 km level with a peak value of 0.40 $ms^{-1}$ at the level of 4 km and decreased linearly to 0 $ms^{-1}$ at the levels of 0 and 6 km.

### 2. *Numerical Experiments*

The numerical experiments are summarized in Table 1. In the control experiment, we applied the new microphysics version developed by Tripoli (1987) with improved aggregation model, in which the diagnosed aggregation efficiency (Eq. 6) was used in the temperature range of 0° ~ −13℃ and Hallgren and Hosler's results used under −13℃ as described in Section II. Sensitivity experiment 1 used the microphysics model of version 5 of RAMS, same as used as control experiment in Cotton et al. (1986). The microphysics model in sensitivity ex-

periment 2 is same with control experiment except for different aggregation efficiency.

**Table 1.** The Numerical Simulation Experiments

| Simulation experiment | Microphysics model | Collection efficiency of ice particles |
|---|---|---|
| Control experiment | New version | $0°\sim-13℃$: $E(T_s)=10^{0.063T_s+0.235}$<br>$T<-13℃$: $E(T_s)=Min[10^{0.035T_s-0.7}, 0.2]$ |
| Sensitivity Exp. 1 | Version 5 | $-12°\sim-15℃$: $E(T_s)=1.4$<br>Otherwise: $E(T_s)=Min[10^{0.035T_s-0.7}, 0.2]$ |
| Sensitivity Exp. 2 | New version | $-12.5°\sim-15.5℃$ and saturation for water:<br>$E(T_s)=1.4$ Otherwise: $E(T_s)=0.3$ |

## V. DYNAMICAL AND THERMODYNAMICAL PROPERTIES OF THE SIMULATED MESO-$\beta$ SCALE CONVECTIVE CLOUD SYSTEM

The control experiment revealed the general properties of the convective cloud system. The dynamical and thermodynamical characteristics of the simulated convective cloud system in the control experiment are described briefly as follows:

### 1. *Vertical Motion*

The time–height cross section of vertical motion (Fig. 3) shows that the meso $-\gamma$ scale convection is basically unsteady. The main convective cells developed in a time interval of about 30 min. The convective cores located at 7.5–8.5 km levels with peak updraft values of 15.0, 20.5, 19.5 and 19.0 $ms^{-1}$ at about 30, 60, 90 and 135 min of simulation time, respectively. The convection weakened after 135 min and dissipated at about 165 min. The meso-$\beta$ scale cloud system exhibited characteristics of a multi–celled convective storm for a period of 3 h as shown in Fig. 4. In the initiation stage, a small convective cell with a peak updraft of 4.0 $ms^{-1}$ formed by 15 min of simulation time at 3 km level, 2 km to the right of domain center. As times advanced, the convective cell rapidly developed to a much stronger one and began to lean more markedly at upper levels. By 30 min, its peak vertical velocity value reached 12.0 $ms^{-1}$ at 7 km level. The ice–phase processes at that level have been active, which probably has an important effect to the developing of strong convection as well as vapor condensation. When the convective cell alofted to the upper levels at about 45 min, it moved to about 8 km to the right of center under the influence of upper levels south–western jet current, and the peak value of vertical velocity reached to 14 $ms^{-1}$ at about 8 km level (Fig. 4a). At the same time, two new convective cells developed with the peak values of 6.0 $ms^{-1}$ at the low levels near the center of domain. These two new cells mainly caused by the convergence of low level wind as well as the first one at the initiated time. They reached their strongest status at about 75 min of simulated real time with a maximum updraft value of 18 $ms^{-1}$. The fourth strong convective cell formed at the left side of the cloud system, 12 km to the left of domain center. It developed much fast than that of the previous cells. In a short range of 15 min it reached its peak updraft value of 16 $ms^{-1}$ at about 8 km level, 10 km to the left of the domain center (Fig. 4c). In the low levels, a new convective cell developed at the location of 18 km to the right of domain center with an updraft value of 10 $ms^{-1}$. After a half hour, the cell reached its strongest updraft value of 12 $ms^{-1}$ at about 9 km level. At the same time an another convective cell developed at mid–levels near the center of domain and reached its strongest status at 135 min, which peak updraft value was 18 $ms^{-1}$ as shown in

Fig. 4c. The convective action was beginning to decay after 135 min of simulated real time.

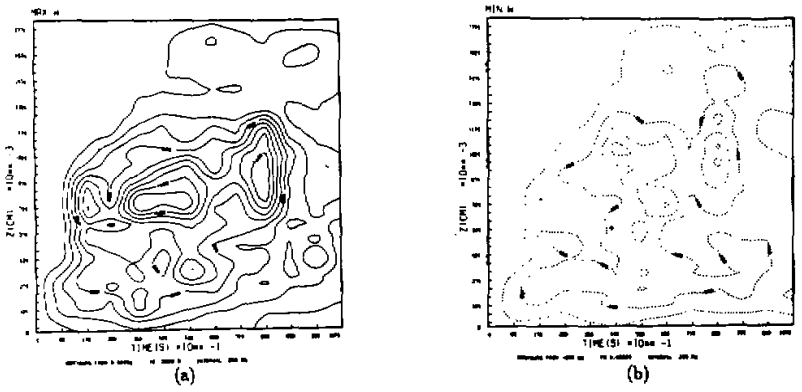


Fig. 3. Time–height cross–section of peak vertical velocity field. The contour interval is 2 $ms^{-1}$. (a)Peak value contours of updraft velocity, (b) Peak value contours of downdraft velocity.

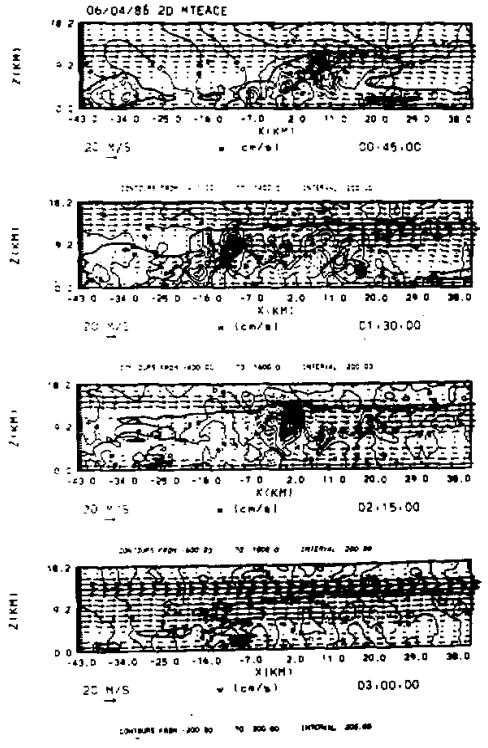


*Fig. 4. Wind vector flow field and contours of vertical velocity at simulated real time of (a) 45 min, (b) 90 min, (c) 135 min, and (d) 180 min. The wind vector is relative to the 15 $ms^{-1}$ storm system motion. The solid lines represent the upward motion and the dashed lines represent the downdraft motion. The contour interval is 2 $ms^{-1}$.*

Several small and weaker convective cells with peak updrafts not stronger than 6 $ms^{-1}$ still developed and maintained to certain range of time at mid–upper levels. The convective action was completely calm down at the simulated real time of 180 min. It is noted from Fig. 4 that the interaction of the low level front to rear flow and mid–level rear inflow in the convective region prompted the form of the main convective cells on the left hand of the cloud system. By the main updraft, a downdraft developed at about 8 km level with weaker values of 6–8 $ms^{-1}$. The air flow at the mid–upper levels exhibited a wave characteristics implying that the gravity wave created as a result of meso–$\beta$ scale convective overturning turned to affect the air motion structure on the larger meso–$\beta$ scale in the troposphere and prompted the formation of the multi–cells storm. The downdraft is weak under the main convective cell since the air is moist in the lower layer, so the effect of evaporation of raindrop may not be evident. The fact that the strong convective activity concentrated at the mid–upper troposphere suggests that the ice–phase process is important to the evolution of the convective system as emphasized by Willoughby et al. (1984) in the simulation of hurricane.

2. *Horizontal Motion*

All the values of horizontal velocity are relative to the moving frame of the simulated cloud system (Figure omitted). In the front side of the mature storm system, inflow mainly concentrated in the low levels, and the outflow is over the mid–upper levels. the mid–level rear inflow evoluted in the mature stage of the storm system. A weaker rear outflow has been found at the upper levels. An upper jet current with peak values larger than 20 $ms^{-1}$ is prevalent above the cloud top. By 45 min, an anvil cloud beginning to form and spreaded downwind under the influence of the upper jet current. After 135 min, the upper jet intensified up to 32 $ms^{-1}$ or more and merged with the mid–level rear inflow which suppressed the convection and resulted in the dissipating of the storm system.

3. *Perturbation Pressure*

As the convection developing, the negative perturbation pressure formed and intensified in the lower layer beneath 5 km level after a half hour (Figure omitted). The largest negative perturbation pressure value of 7.5 hPa is found on lower boundary at 75 min. Another lowest perturbation pressure center formed at the end of simulation time. Above 7 km level, the positive perturbation pressure formed by a half hour and suspended to the end of simulation time. Three meso high centers with the peak values of 2.1, 1.6 and 2.6 hPa formed at the levels from 8 to 11 km at 90, 120 and 150 min, respectively.

The perturbation pressure field (Figure omitted) exhibited that a small meso–high caused by the initial cold downdraft maintained in the first half hour of simulation time near the center of domain with a peak value of 2.0 hPa. A meso–low of −1.5 hPa formed by the first half hour at low levels, 9 km to the center of domain at 30 min of simulation time, and intensified up to −7.5 hPa at 75 min. The meso–low extended to the upshear side and covered the entire domain beneath the 7.5 km level after 90 min of the simulated real time, whereas the intensity of the perturbation low pressure weakened and maintained its intensities of −3.5 to −5.5 hPa for about 75 min. At the end of simulation, the perturbation low pressure reached its peak value of −8.0 hPa. A weaker high pressure area developed near cloud top after 45 min. The meso–high reached its peak value of 2 hPa at 90 min, which located on the upshear side of cloud system at the 8 to 11 km levels.

4. *Perturbation Potential Temperature*

In the entire period of storm system developing and evolution, middle–upper troposphere (from 5 to 10 km) is a warm layer (Fig. omitted). Several meso–$\gamma$ scale warm cores were basically associated with the action of strong convective cells, especially in first two hours. During the developing of the convective cloud system at the first hour of simulation, a perturbation potential temperature of 4.0℃ presented in the first convection cell at about 6 km level, slightly lower than that the strongest convection center. By 45 min, a perturbation temperature of 4.0℃ formed out of the cloud in the down–shear side at about 5 km level, which was probably caused by the compensating subsidence out of the cloud. The main warm region still located in the strong convective cell. The warm region extended in the mid–levels as the anvil cloud evolving at 60 min of simulated real time, with a peak anomalous temperature of 8℃ at about 8 km level accompanying with the active convective cells. This anomalous warm region lasted to the end of simulation with peak values ranging from 6 to 8℃. The warm region basically located above the 0℃ level implying that the ice–phase microphysical processes act an important effect on it.

Since the low levels are moist, cooling by evaporation of raindrops in the low levels was not evident and the warm area almost occupied the entire domain beneath the 9 km level. Cooling by cloud top evaporation can be seen from the simulation with peak anomalous values of −10 ° to −14℃.

## VI. MICROPHYSICS OF THE SIMULATED MESO–$\beta$ SCALE CONVECTIVE CLOUD SYSTEM

1. *The Control Experiment*

Fig. 5 illustrated the time series of cloud droplet, rairdrop, graupel, and aggregates mixing ratio. Comparing with Fig. 3, the peak values of raindrop and graupel were basically associated with the strong convective cells. Graupel cores were located just over that of raindrop implying the graupel is the main source of convective rainfall. On the other hand, the variation of the peak aggregate value is much smooth with time, implying aggregates was formed in both stratiform region and convective cells. Here we describe the predicted microphysical structures a little bit detailly:

(1) *Cloud and rain water fields*

The cloud and rain water contents were basically restricted in the warm layer, under the 4.5 km level as expected (see Fig. 5a, b). The highest values of rain water were seen in the main updraft developed at about 30, 60, 90 and 135 min of simulation time as shown in Fig. 3. The contours of cloud water mixing ratio showed that the liquid cloud water content mainly concentrated in the low levels newly generated convective cells as would be expected due to the condensation occurring there, in which the condensation process in the saturation updraft did not exhaust seriously by collection with precipitation particles since which was lack in the newly generated convective cells.

(2) *Pristine crystal and snow crystal fields*

The pristine crystals and snow crystals formed by 30 min above the 0℃ level. During the developing and mature stages, the peak mixing ratio values of these particles reached 1.0–1.5 g $kg^{-1}$ in the stratiform region of the cloud system. The contents of snow crystals were less than 0.5 g $kg^{-1}$ after 150 min when the convective action decaying (Figure omitted).

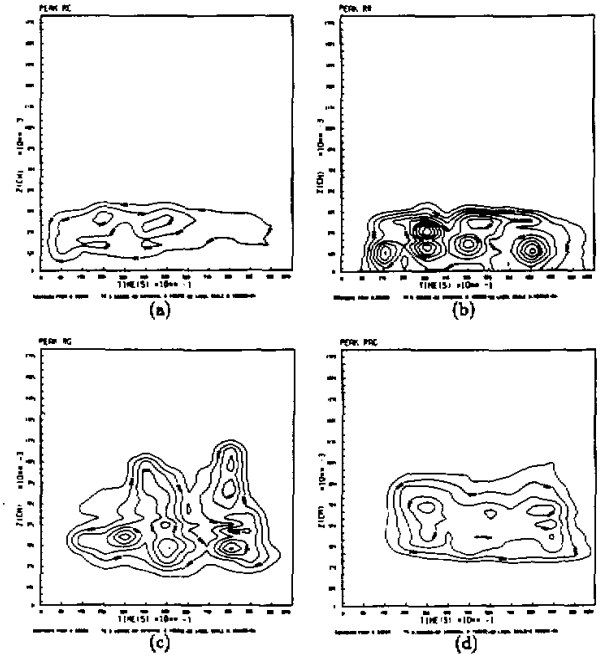


Fig. 5. Time–height cross–section of peak values of various types microphysical variables. (a) cloud droplet, (b) raindrop, (c)graupel, and (d) aggregates. The contour intervals are 1.0 g kg$^{-1}$.

(3) *Graupel particle field*

The predominant formation mechanism of graupel is riming of freezing raindrop, ice crystal and aggregates. The main growth mechanism of graupel is accretion of raindrop and aggregates by graupel particle itself. Both of them are active in the high water content region of cloud droplet and raindrop. So the graupel is primarily concentrated in the strong convective cells which is the main source of the convective rainfall. Contours of graupel mixing ratio are shown in Fig. 6. The peak values of 3.5 and 6.0 g kg$^{-1}$ of it located at the lower part of main convective cells from 4 to 6 km levels in the developing stage of cloud system at about 30 and 60 min, and of 5.5 and 4.5 g kg$^{-1}$ found from 3 to 9 km levels in the mature stage at about 90 and 135 min. After 150 min the graupel was beginning to dissipate as convection decaying.

(4) *Aggregates field*

Aggregation between ice crystals is a main formation mechanism of aggregates. Observational analysis indicated (Yeh et al., 1987) that, in the MCC, most large precipitation particles are graupel and aggregates in the transition region nearby mature convective cell, whereas aggregates predominated in the stratiform region. Aggregation process occurs over a considerable depth and range of temperature in the stratiform region which is the main source of stratiform rainfall. Fig. 7 showed the simulated contours of aggregates mixing ratio. It can be seen from Fig. 7 that the aggregates spread much large extent in space than that of graupel.

Aggregates primarily located in decaying convective cells and stratiform region of the cloud system at the levels from 4 to 8 km with peak values ranging from 2.5 to 4.0 g $kg^{-1}$ in the developing and mature stage of the storm system.

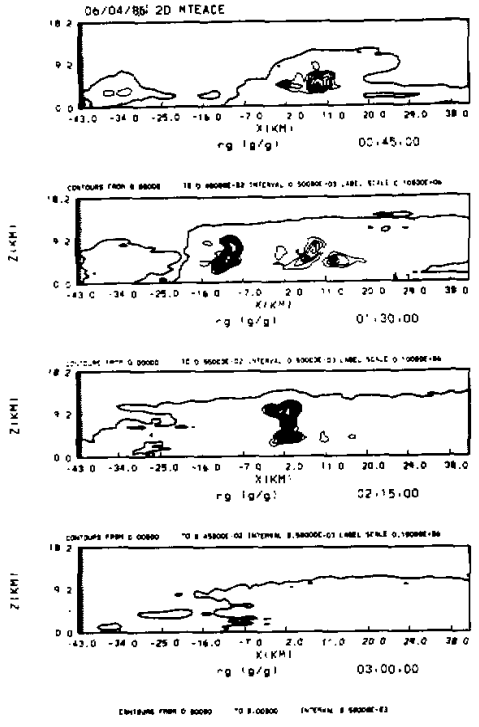


Fig. 6. Contours of graupel particle mixing ratio for the control experiment at (a) 45 min, (b) 90 min, (c) 135 min, and (d) 180 min. The cloud boundary (condensate in excess of 0.01 g $kg^{-1}$) is drawn by a heavy dark line. The vertical axis is height in km above mean sea level and the $x$ axis is horizontal distance from the center of domain in km. The contour interval is 0.5 g $kg^{-1}$.

## 2. *The Sensitivity Experiments*

The sensitivity experiments with various aggregation efficiencies are summarized as follows:

In the sensitivity experiment 1 (see Table 1), we assumed the aggregation collection efficiencies were given from that used as a control experiment in Cotton et al (1986). Fig. 8 illustrated the predicted contours of mixing ratio of various ice–phase particles at 90 min obtained from the sensitivity experiment 1. The ice crystals occupy the entire cold region above the 7 km level in the cloud system with a peak value of 3.0 g $kg^{-1}$ located in the main convective cell around 10 km level, whereas there was almost no any aggregates in the entire cloud system. As the cloud system evolution, the peak value of ice crystal water content reached to 3.5 g $kg^{-1}$. Obviously, the aggregation efficiency selected by version 5 of RAMS is too low.

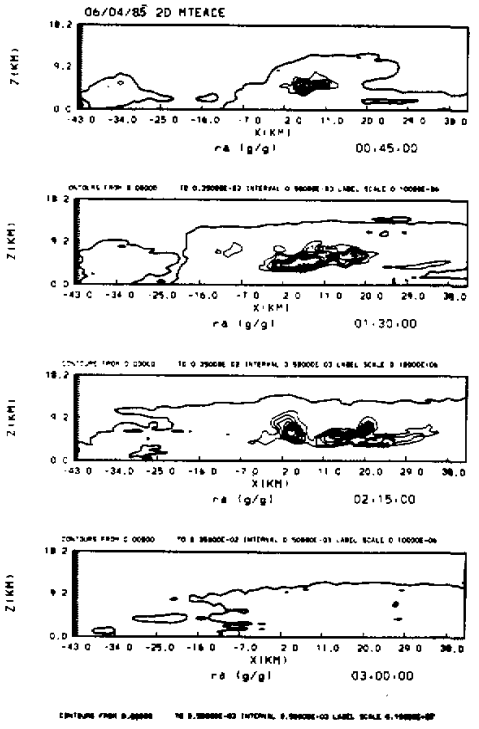


Fig. 7. Same as Fig. 6 except for aggregates.

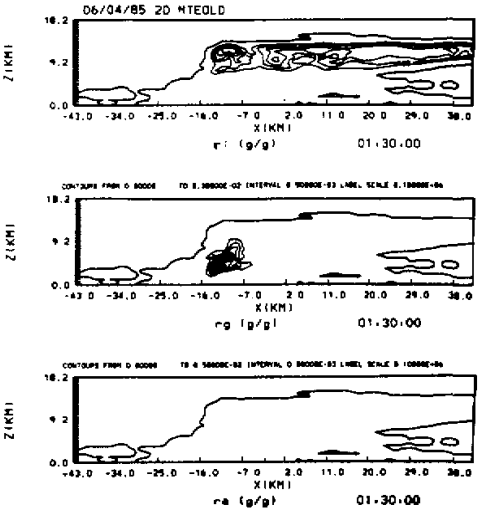


Fig. 8. Ice–phase microphysical structure at 90 min simulation time for sensibility Exp. 1 as shown in Table 1. (a)

Contours of ice crystal mixing ratio, (b) graupel mixing ratio, and (c) aggregates mixing ratio, all contours at intervals of 0.5 g kg$^{-1}$.

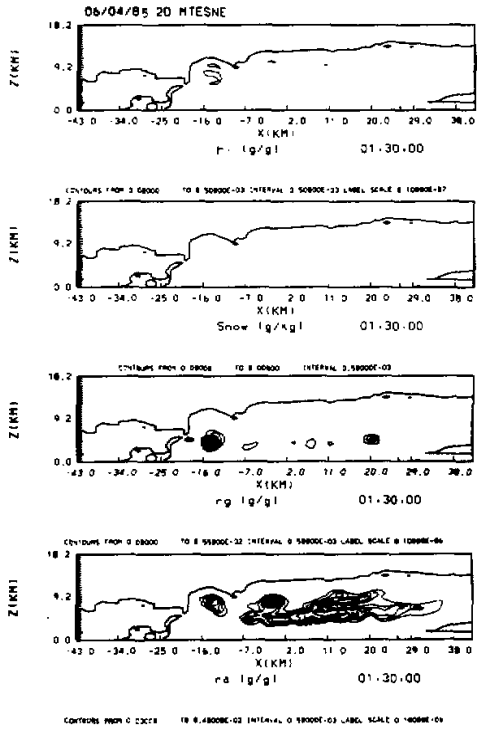


Fig. 9.Same as in Fig. 8 except for sensibility Exp. 2 as shown in Table 1.

Fig. 9 is the same as Fig. 8 except for sensitivity experiment 2 in Table 1, in which the Passarelli's diagnosed constant value 1.4 of aggregation collection efficiency was used over the temperature range $-12.5 - -15.5$℃, and the empirical value 0.3 of Latham and Saunders (1971) was used elsewhere. Compared to Exp. 1, aggregates dominated in the whole cold region of cloud system with a peak value of 4.0 g kg$^{-1}$ around the 8 km level, and pristine crystals and snow crystals were almost totally depleted. At 135 min, the peak value of aggregates reached 5.0 g kg$^{-1}$ in the decaying convective cell near 8 km level. The aggregation efficiencies used in this case is too large.

The results of the control experiment is given in Fig. 10. Here the microphysical structure using the diagnosed aggregation efficiency seems to be better. Pristine crystals and snow crystals were found mainly above 7 km level with peak values of 1.0 g kg$^{-1}$. Graupel concentrated in the strong convective cell and extend in a deep layer from 3 to 9 km with peak value of 5.5 g kg$^{-1}$ beneath the strongest convection core which composed the main source of convective rainfall. Some graupel is found in the decaying convective cells. Aggregates primarily extended in the stratiform region and decaying convective cells in the layer from 4 to 8 km composing the source of stratiform rainfall. The peak aggregates mixing ratio of 3.5 g kg$^{-1}$ is located at the lower levels near the melting layer, which is consistent qualitatively with the ob-

servations that aggregation starts at the upper and colder levels but becomes more efficient near the melting layer (Yeh, et al., 1987).

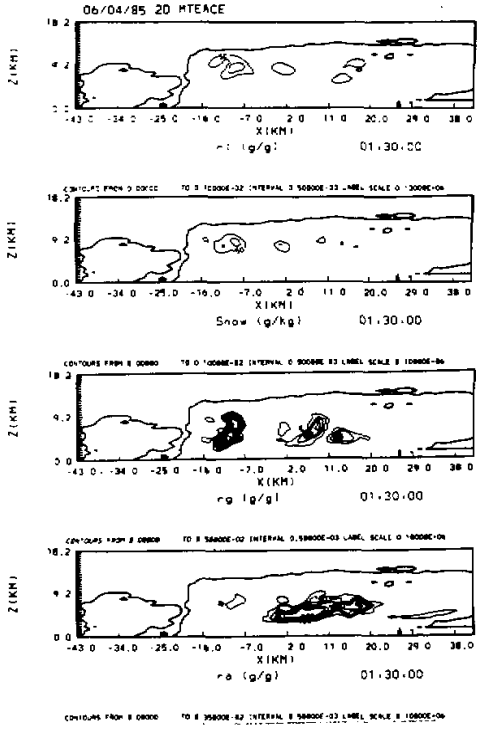


Fig. 10. Same as in Fig. 8 except for control experiment as shown in Table 1.

## VII. CONCLUSIONS

1. The meso–$\gamma$–scale convective phenomena are basically unsteady under the situation of strong shear of wind at low–levels, while the meso–$\beta$–scale convective system is maintained up to 3 hours or more. The meso–$\beta$–scale cloud system exhibits characteristics of a multi–celled convective storm. The main convective cells (meso–$\gamma$–scale) develop in it by a time interval of about 30 min. The fact that the strong convective activity concentrated at mid–upper troposphere suggests that the ice–phase process is important to the development and evolution of the convective system.

2. Pressure perturbations depict a meso–low after a half hour in the low levels. As the cloud system evolution,the meso–low intensifies and extends to the upshear side and covers the entire domain beneath 7.5 km level with the peak values from 5 to 8 hPa.

3. Temperature perturbations depict a cold region in the low levels at the first hour, and a much stronger cold layer caused by cloud top evaporation at the upper levels around the cloud top level after one hour. In the middle levels, a warm region is present through the entire simulation period. The warm cores with peak values from 4.0 to 8.0℃ are basically associated with strong convective cells.

4. Simulation of microphysics exhibits that graupel is primarily concentrated in the

strong convective cells forming the main source of convective rainfall after one hour, and aggregates are mainly located in the stratiform region and decaying convective cells which produce the stratiform rainfall. Riming of ice crystals is the predominant precipitation formation mechanism in the convective cells, whereas aggregation of ice crystals is the predominant one in the stratiform region, which is consistent with observations.

5. Sensitivity experiments show that the microphysical structures of the convective cloud system can be simulated better by the new version of the parameterized microphysics with the diagnosed collection efficiencies.

This research was funded by the National Science Foundation under Grant #ATM-8512480 and by the Army Research Office under contract #DAAL03-86-K-0175. We would like to thank Brenda Thompson for her help in processing the manuscript, and Lucy McCall for her drafting work. All computations were performed on the National Center for Atmospheric Research (NCAR) Cray X-MP48 computer. NCAR is supported by the National Science Foundation of the United States.

REFERENCES

Chen Sue (1986), Simulation of the stratiform region of a mesoscale convective system, M.S. Thesis, Colorado State University, Fort Collins, CO 80523, 107pp.

Cotton, W.R., M.A. Stephens, T. Nehrkorn, and G.J. Tripoli (1982), The Colorado State University cloud / mesoscale model-1982, Part II: An ice phase parameterization, *J. Rech. Atmos.*, **16:** 295-320.

Cotton, W.R., G.J. Tripoli, R.M. Rauber, and E. A. Mulvihill (1986), Numerical simulation of the effects of varying ice crystal nucleation rates and aggregation processes on orographic snowfall, *J. Clim. Appl. Meteor.*, **25:** 1658- 1680.

Fortune, M.A., and R.L. McAnnelly (1986), The evolution of two mesoscale convective complexes with different patterns of convective organization, Preprints of Joint Session, *23rd Conference on Radar Meteorology and Conference on Cloud Physics*, AMS, Snowmass, Colorado, J175-178.

Hallgren, R.E., and C.L. Hosler (1960), Preliminary results on the aggregation of ice crystals,, *Geophys. Monogr., Am. Geophys. Union*, **5:** 257-263.

Heymsfield, A.J., and D.J. Musil(1982), Case study of a hailstorm in Colorado, Part II: Particle growth processes at midlevels deduced from in-situ measurements, *J. Atmos. Sci.*, **39:** 2847-2866.

Hobbs, P.V., S. Chang, and J.D. Locatelli (1974), The dimensions and aggregation of ice crystals in natural cloud, *J. Geoph. Res.*, **79:** 2199-2206.

Hosler, C.L., D.C. Jensen, and L. Goldshlak (1957), On the aggregation of ice crystals to form snow, *J. Met.*, **14:** 415-420.

Houze, R.A., Jr., and D.D. Churchill (1984), Microphysical structure of winter cloud clusters, *J. Atmos. Sci.*, **41:** 3405-3411.

Jorgensen, D.P. (1984), Mesoscale and convective-scale characteristics of mature hurricanes, Ph. D. dissertation, Colorado State University, Fort Collins, CO 80523, 189pp.

Jiusto, J.E. (1971), Crystal development and glaciation of a supercooled cloud, *J. Rech, Atmos.*, **5:** 69-85.

Latham, J., and C. P. R. Saunders (1971), Experimental measurements of the collection efficiencies of ice crystals in electric fields, *Quart. J. Roy. Meteor. Soc.*, **96:** 257-265.

Lo, K.K., and R.E. Passarelli, Jr. (1982), The growth of snow in winter storm: An airborne observational study, *J. Atmos. Sci.*, **39:** 697-706.

Matejka, T.J., R.A. Houze, Jr., and P. V. Hobbs (1980), Microphysics and dynamics of clouds associated with mesoscale rainbands in extratropical cyclones, *Quart. J. Roy. Met. Soc.*, **106:** 29-56.

Passarelli, R.E., Jr. (1978), Theoretical and observational study of snow-size spectra and snowflake aggregation efficiencies, *J. Atmos. Sci.*, **35:** 882-889.

Rauber, R.M. (1987), Characteristics of cloud ice and precipitation during wintertime storms over the mountains of

Northern Colorado, *J. Climate and Appl. Meteor.*, **26**: 488–524.

Steward, R.E., J. D. Marwitz, J.C. Pace, and R.E. Carbone (1984), Characteristics through the melting layer of stratiform clouds, *J. Atmos. Sci.*, **41**: 3227–3237.

Tripoli, G.J., and W.R. Cotton (1982), The Colorado State University three–dimensional cloud / mesoscale model–1982, Part I: General theoretical framework and sensitivity experiments, *J. Rech. Atmos.*, **16**: 185–220.

Willoughby, H.E., Han–Liang Jin, S.J. Lord, and J.M. Piotrowicz (1984), Hurricane structure and evolution as simulated by an axisymmetric nonhydrostatic numerical model, *J. Atmos. Sci.* **41**: 1169–1186.

Yeh Jiadong, Fan Beifen, M.A. Fortune, and W.R. Cotton (1987), Comparison of the microphysics between the transition region in a mesoscale convective complex, Third Conference on Meso–scale Processes, 21–26 August, 1987, Vancouver, D.C., Canada, 188–189.